Environmental Modeling

Atmospheric mercury outflow from China and interprovincial trade

Long Chen, Sai Liang, Yanxu Zhang, Maodian Liu, Jing Meng, Haoran Zhang, Xi Tang, Yumeng Li, Yindong Tong, Wei Zhang, Xuejun Wang, and Jiong Shu

Environ. Sci. Technol., **Just Accepted Manuscript** • DOI: 10.1021/acs.est.8b03951 • Publication Date (Web): 29 Oct 2018

Atmospheric mercury outflow from China and interprovincial trade

Long Chen[1,2], Sai Liang[3], Yanxu Zhang[4], Maodian Liu[5], Jing Meng[6], Haoran Zhang[5], Xi Tang[1,2], Yumeng Li[3], Yindong Tong[7], Wei Zhang[8], Xuejun Wang[5,*] and Jiong Shu[1,2,*]

[1] Key Laboratory of Geographic Information Science (Ministry of Education), East China Normal University, Shanghai, 200241, China

[2] School of Geographic Sciences, East China Normal University, Shanghai, 200241, China

[3] State Key Joint Laboratory of Environment Simulation and Pollution Control, School of Environment, Beijing Normal University, Beijing, 100875, China

[4] School of Atmospheric Sciences, Nanjing University, Nanjing, Jiangsu, 210023, China

[5] Ministry of Education Laboratory of Earth Surface Process, College of Urban and Environmental Sciences, Peking University, Beijing, 100871, China

[6] Department of Politics and International Studies, University of Cambridge, Cambridge CB3 9DT, UK

[7] School of Environmental Science and Engineering, Tianjin University, Tianjin 300072, China

[8] School of Environment and Natural Resources, Renmin University of China, Beijing, 100872, China

Abstract

Mercury (Hg) is characterized by the ability to migrate between continents and adverse effects on human health, arousing great concerns around the world. The transboundary transport of large anthropogenic Hg emissions from China has attracted particular attention, especially from neighboring countries. Here, we combine an atmospheric transport model, a mass budget analysis, and a multiregional input-output model to simulate the atmospheric Hg outflow from China and investigate the impacts of Chinese interprovincial trade on the outflow. The results show outflows of 423.0 Mg of anthropogenic Hg, consisting of 65.9% of the total Chinese anthropogenic emissions, from China in 2010. Chinese interprovincial trade promotes the transfer of atmospheric outflow from the eastern terrestrial boundary (–6.4 Mg $year^{-1}$) to western terrestrial boundary (+4.5 Mg $year^{-1}$) and a net decrease in the atmospheric outflow for the whole boundary, reducing the chance of risks to foreign countries derived from transboundary Hg pollution from China. These impacts of interprovincial trade will be amplified due to the expected strengthened interprovincial trade in the future. The synergistic promotional effects of interprovincial trade versus Hg controls should be considered for reducing the transboundary Hg pollution from China.

1. Introduction

Mercury (Hg) is a global toxic pollutant that is characterized by long distance atmospheric transport, which contributes to its ability to migrate across the oceans between continents.[1,2] Owing to dry and wet scavenging, Hg can be deposited in terrestrial and aquatic ecosystems. Methylmercury (MeHg) can be formed via the methylation and bioaccumulation of Hg in food webs after deposition, adversely affecting human health, such as by causing neurocognitive deficits in children and cardiovascular problems in adults.[3-7] Several human health disasters have already occurred owing to MeHg exposure (e.g., Minamata disease),[8] promoting the launch of the *Minamata Convention on Mercury*.[9] The convention focuses on transboundary Hg pollution and controls around the world.

China is the largest Hg emitter in the world, releasing approximately 33% of the global total anthropogenic emissions to the air each year.[1,10,11] The transboundary transport of large Hg emissions outside China have aroused great concerns from all countries of the world, especially neighboring countries. For instance, combining monitoring data and meteorological data, scholars suggested that high Hg concentrations observed at Mt. Fuji and Cape Hedo in Japan might be related to the transboundary transport of Hg from China.[12,13,14,15] These concerns require studies focusing on atmospheric Hg outflows from China and the subsequent impacts on neighboring regions. Previous studies have illustrated that anthropogenic emissions from East Asia significantly contribute to Hg deposition over the rest of the world. For instance, 70–75% of the total emissions from East Asia were transported outside the region, and the maximum occurred in spring and early summer, contributing 20–30% of the total

atmospheric deposition over remote regions.[16,17] Anthropogenic emissions from East Asia were the primary sources for deposition over global oceans,[2,18] especially the Arctic.[19,20] However, atmospheric Hg outflows from China and the associated impacts on neighboring deposition have not been investigated.

China is a vast country with substantial disparities in socioeconomic development across provinces, such as in the consumption of resources and energy, population growth, and lifestyles, resulting in frequent and substantial interprovincial trade. Interprovincial trade separates production activities and final consumption and subsequently induces embodied air, water and soil pollution.[21-24] The atmospheric Hg emissions embodied in interprovincial trade have been well-documented in China, resulting in a comprehensive virtual atmospheric Hg emission network among Chinese provinces.[25-27] The network shows that a large amount of Hg emitted from inland provinces is caused by the final consumption in coastal provinces.[25,26] In addition to Hg emissions, previous studies also found that 32% of atmospheric deposition over China was embodied in interregional trade and that deposition was considerably redistributed by this trade.[28] Considerable impacts of interprovincial trade on atmospheric Hg emissions and deposition within China have been verified by previous studies, but impacts of interprovincial trade on Hg transport outside China are poorly understood.

In this study, we combine an atmospheric transport model, a mass budget analysis, and a multiregional input-output model to simulate the atmospheric outflow of anthropogenic Hg emitted from human activities in China and subsequent deposition over neighboring seas and lands and investigate the impacts of Chinese interprovincial trade on Hg outflow and deposition. Accordingly, suggestions on controlling transboundary Hg

84 pollution from China are proposed. The findings in our study are relevant to efforts on
85 international collaboration to reduce transboundary Hg pollution.
86
87 **2. Materials and Methods**
88 **2.1. Study area and associated anthropogenic emissions**
89 The study domain is located from 70°E to 150°E and 11°S to 55°N, which represents
90 the East Asian domain. This area covers China and other parts of East Asia, such as Japan,
91 the Republic of Korea, India, Indonesia, Vietnam, Thailand, and Mongolia (Figure S1).
92 To evaluate the impacts of interprovincial trade on foreign deposition, we choose several
93 representative neighboring seas and lands that border on terrestrial China or that are
94 located offshore and classify these regions into five groups according to their locations,
95 namely, the Chinese coastal seas, Japan-Korea, Southeast Asia, South Asia, and
96 Mongolia (*SI Dataset S1*; Figure S1). To evaluate the impacts of interprovincial trade on
97 atmospheric outflow, we divide the whole geographic boundary of China into the eastern
98 terrestrial boundary and western terrestrial boundary. The eastern terrestrial boundary
99 includes all the coastlines and national boundaries located in the northeast provinces.
100 (Figure S1).
101 Human activities, such as coal combustion, nonferrous metal smelting and cement
102 production, emit large quantities of Hg to the atmosphere each year. In this study,
103 anthropogenic emissions from China from the producer perspective (i.e., production-
104 based emissions) are referenced from our previous work,[28] which compiled a Chinese
105 emission inventory in 2010 by multiplying energy usage and product yields by the
106 respective emission factors. The anthropogenic emissions are distributed as point and

107 nonpoint sources in terms of industrial productivity and gridded population density.
108 Seasonal variations have not been evaluated for the emissions due to data unavailability.
109 The production-based emissions for each province and each economic sector are given in
110 *SI Dataset S4* and *Dataset S5*, respectively. Anthropogenic emissions from other parts of
111 Asia are referenced from the AMAP/UNEP (Arctic Monitoring and Assessment
112 Programme/United Nations Environment Programme) global anthropogenic emission
113 inventory in 2010.[1]
114
115 **2.2. Evaluation of trade-induced emissions**
116 The calculation of the interprovincial trade-induced Hg emissions is based on an
117 environmentally extended multiregional input-output (EE-MRIO) analysis of the
118 interactions between different economic sectors (*SI Dataset S2*) and provinces in China
119 multiplied by sector-specific emission intensities. The MRIO table of China in 2010
120 developed by Liu et al.[29] is used in this study to evaluate interprovincial trade-embodied
121 Hg emissions among Chinese provinces. A brief introduction of the MRIO approach is
122 shown as follows:
123 $$\mathbf{X} = (\mathbf{I} - \mathbf{A})^{-1}\mathbf{Y} \quad (1)$$
124 where **X** is a vector of the total monetary output for different sectors, **Y** is a vector of
125 final demand for different sectors, including final consumption (**F**) (i.e., urban household
126 consumption, rural household consumption, government consumption and investment)
127 and international export (**E**). **I** represents the unsity matrix, and **A** denotes the direct
128 requirement coefficient matrix. Element a_{ij} in matrix **A** is defined as the intermediate

input from sector *i* to the production of a unit output for sector *j*. $(\mathbf{I} - \mathbf{A})^{-1}$ is the *Leontief inverse matrix,* which is the foundation of the MRIO approach.

Multiplying by the direct emission intensity vector (ψ) for equation (1), we calculate sector- and province-specific consumption-based emissions with the corresponding final consumption **F**. We define ψ_0 as a vector with zero for a given sector or province but the direct emission intensity for other sectors or provinces. Through multiplying by the vector, we calculate emissions embodied in imports (EEI) for the given sector or province with its corresponding final consumption **F** (eq 2). The hats over ψ_0 and **F** mean diagonalizing vectors of ψ_0 and **F**. The correspondence relationships between direct emission sources and sectors of the Chinese MRIO table are shown in *SI Dataset S3.*

$$\mathrm{EEI} = \hat{\boldsymbol{\psi}}_0(\mathbf{I} - \mathbf{A})^{-1}\hat{\mathbf{F}} \qquad (2)$$

To evaluate the impacts of interprovincial trade, we set up a hypothetical scenario with an absence of interprovincial trade. We assume the trade partners could produce the same goods which are originally involved in interprovincial trade locally, and then EEI of a given province are assumed to be relocated from its trade partners to the province. Similar to previous studies,[30,31] the assumed relocation of EEI reveals the same technologies when producing the same goods between trade partners and is used to evaluate the difference between existence and absence of interprovincial trade. The results of trade-induced emissions are shown in *SI Dataset S4* and *Dataset S5*. Meanwhile, the net emission flows induced by interprovincial trade is shown in Figure S2.

2.3. Simulation of atmospheric Hg outflow and deposition

The GEOS-Chem chemical transport model (version 9-02; http://geos-chem.org) is used to simulate atmospheric Hg deposition over the study area and atmospheric Hg outflow from China. The model is a 3-D atmosphere model that is integrated to a 2-D surface slab ocean and a 2-D soil reservoir for Hg cycle.[32-34] Three Hg species, namely, elemental Hg (Hg^0), divalent Hg (Hg^{II}) and particulate Hg (Hg^P), are tracked in the model. Hg^0 can be oxidized to Hg^{II} by Br atoms, while Hg^{II} can be reduced to Hg^0 under light in cloud droplets.[33] Meanwhile, the balance of gas-particle partitioning is maintained between Hg^{II} and Hg^P.[35] Dry deposition and wet scavenging of atmospheric Hg in the model follow the resistance-in-series scheme from Wesely[36] and the scheme from Liu et al.,[37] respectively. The model is driven by the assimilated meteorological fields from the Goddard Earth Observing System (GEOS-5) conducted by the NASA Global Modeling and Assimilation Office (GMAO).

Using the method presented in our previous work,[28] a nested model can be conducted over East Asia at native horizontal resolution of 1/2° × 2/3° and 47 vertical levels from the surface to 0.01 hPa. Before performing the nested simulation, a global 4° × 4.5° resolution simulation is conducted first for lateral boundary conditions of the nested simulation. The global simulation is driven by emissions combining the Chinese emission inventory in China and the AMAP/UNEP global anthropogenic emission inventory outside China.[1] The nested model's performance has been evaluated against a series of observations in our previous work. In this study, we run the nested model with two emission scenarios representing existence and absence of interprovincial trade, respectively, in 2010 under an initial spin-up of the last three months in 2009. The lateral boundary conditions are provided by

global simulations during 2008–2010. The outputs are archived monthly and are used to illustrate seasonal variations in atmospheric outflow and deposition.

2.4. Calculation of regional Hg mass budget

The atmospheric Hg outflow from China is estimated by calculating Hg mass budget for China using the GEOS-Chem simulation results for each modeling month. We use a schematic for the regional mass budget calculation proposed by Lin et al.[16] In general, the change in atmospheric Hg burden within a region over a simulation period can be influenced by the Hg mass entering and leaving the region via atmospheric transport, atmospheric Hg emissions, and atmospheric Hg deposition via dry and wet scavenging. Meanwhile, the net change in atmospheric Hg burden within a region also equals the difference between the atmospheric Hg burden at the beginning and at the end of the simulation period. The schematic can be expressed by the following equations:

$$FB - IB = IM - OM + E - D \quad (3)$$

$$OF = OM - IM = E - D - FB + IB \quad (4)$$

where FB is the atmospheric burden within the region at the end of the simulation period and IB is the atmospheric burden within the region at the beginning of the simulation period. IM, OM, E and D represent the Hg mass that enters the region, the Hg mass that leaves the region, the atmospheric emissions in the region and the atmospheric deposition in the region over the simulation period, respectively. OF represents the net atmospheric outflow from the region via atmospheric transport, which can be defined as the difference between the Hg mass leaving the region and entering the region. All the terms are in Mg per period. In this study, we evaluate all the terms driven by Chinese anthropogenic

196 emissions to illustrate the impacts of human activities in terrestrial China on neighboring
197 seas and lands.
198
199 **3. Results and Discussion**
200 **3.1 Atmospheric Hg outflow from China**
201 In 2010, human activities in China totally release 641.7 Mg Hg to the air, 218.7 Mg
202 of which is deposited in terrestrial China and 423.0 Mg of which is transported outside
203 terrestrial China (Figure 1). The atmospheric outflow consists of 65.9% of the total
204 Chinese anthropogenic emissions, and the large contribution indicates that China serves
205 as both an important Hg emitter and an important Hg exporter globally. For the whole
206 year, the atmospheric burden over China driven by Chinese anthropogenic emissions
207 remains nearly constant.
208 Moreover, seasonal variations are observed for atmospheric Hg deposition and
209 outflow for China (Figure 1b). In summer months, large near-source deposition occurs in
210 China due to the large amount of rain, which increases atmospheric deposition over
211 terrestrial China and subsequently reduces atmospheric outflow from terrestrial China.
212 The largest deposition (24.2 Mg $month^{-1}$) and smallest outflow (27.7 Mg $month^{-1}$) occur
213 in August. In winter months, in contrast, the atmospheric deposition over terrestrial China
214 decreases and atmospheric outflow increases subsequently due to lower amount of rain
215 and limited scavenging in winter in China. The smallest deposition (13.1 Mg $month^{-1}$)
216 and largest outflow (41.4 Mg $month^{-1}$) values occur in February. The seasonal difference
217 reveals that human activities in China contribute more to domestic Hg pollution in
218 summer months and neighboring Hg pollution in winter months.

3.2 Impacts of interprovincial trade on the atmospheric outflow

Human activities in China release a total of 641.7 Mg Hg to the air in 2010, 503.0 Mg Hg of which is related to the final consumption of the Chinese population (*SI Dataset S4*). The remaining mass is related to non-economic activities (i.e., residential coal consumption and the use of Hg-added products) and foreign consumption. For a specific province in China, the final consumption includes consumption of local goods and imported goods, inducing local emissions (i.e., on-site emissions embodied in the own consumption of the province) and emissions in other provinces that are involved in interprovincial trade (i.e., EEI), respectively. For the whole nation, the imports of goods and services induce 227.6 Mg $year^{-1}$ Hg emissions. Meanwhile, among the EEI, 85.6 Mg $year^{-1}$ Hg is embodied in net interprovincial trade, which represents the net transfer from embodied Hg importers to embodied Hg exporters within China (*SI Dataset S4*).

Figure 2 illustrates the impacts of interprovincial trade on the net atmospheric Hg outflow from the whole boundary of China. Due to Chinese interprovincial trade, approximately 1.9 Mg $year^{-1}$ of net Hg would have been transported outside China, but it is deposited in terrestrial China (1.6 Mg $year^{-1}$) and stored in the atmosphere (0.3 Mg $year^{-1}$). Most of the embodied Hg importers are developed provinces in China located on the southeast coast, while most of the embodied Hg exporters are developing provinces in China located in inland regions. As a result of interprovincial trade, emissions flow from the southeast coast to inland regions (Figure S2), which was also reported by previous studies.[26,28] These emissions are easily deposited in terrestrial ecosystems and stored in

241 the atmosphere over terrestrial China due to the greater distance from the terrestrial
242 boundaries.

243 Compared to the small net change for the whole boundary, interprovincial trade
244 contributes more to the change in spillover channels. The emission flows from the
245 southeast coast to inland regions during interprovincial trade contribute to the decrease in
246 spillover from the eastern terrestrial boundary and the increase from the western
247 terrestrial boundary (Figure 3). The decrease from the eastern terrestrial boundary is
248 estimated to be –6.4 Mg year^{-1} consisting of 7.5% of the emissions embodied in net
249 interprovincial trade, while the increase from the western terrestrial boundary is estimated
250 to be +4.5 Mg year^{-1}. The decrease in spillover from the eastern terrestrial boundary
251 contributes to the decrease in atmospheric deposition over the seas and lands leaving the
252 eastern terrestrial boundary, such as the Chinese coastal seas, the Sea of Japan, Japan-
253 Korea, and some regions in Southeast Asia (Figure 3). However, the increase in spillover
254 from the western terrestrial boundary contributes to the increase in atmospheric
255 deposition over the lands outside the western terrestrial boundary, such as Mongolia,
256 South Asia, and some regions in Southeast Asia (Figure 3).

257 The transfer of atmospheric outflow from the eastern terrestrial boundary to western
258 terrestrial boundary is a highly significant change in transboundary Hg pollution from
259 China. As we know, human MeHg exposure stems almost entirely from the consumption
260 of seafood, such as fish and shellfish harvested from marine regions.[38-40] Thus, marine
261 regions are the critical receptors of Hg posing health risks to human beings.[3,41,42]
262 Accordingly, the decrease in atmospheric outflow from the eastern terrestrial boundary
263 and the subsequent decrease in atmospheric deposition over the seas outside the eastern

terrestrial boundary may reduce the Hg in seafood harvested from the seas, which can reduce the MeHg exposure risks for humans who rely heavily on marine-based diets, such as the populations of Japan and the Republic of Korea. In general, through the transfer of atmospheric outflow between different boundaries, interprovincial trade reduces the chance of risks to foreign countries derived from transboundary Hg pollution from China.

Moreover, the transfer of atmospheric outflow from the eastern terrestrial boundary to western terrestrial boundary is characterized by significant seasonal differences (Figure 3). The seasonal differences are attributed to the prevailing wind directions of the East Asian Monsoon (Figure S3). In the autumn and winter months, seasonal winds from Siberia to the Northwest Pacific bring atmospheric Hg from the southeast coast of China to the downwind seas outside the eastern terrestrial boundary, and the decrease in deposition occurs over the seas due to exported emissions outside the southeast coast of China (Figure S3a and S3d). Meanwhile, the seasonal winds also bring atmospheric Hg from southwest China to downwind regions in South Asia, and the increase in deposition occurs over these regions due to imported emissions into southwest China (*SI Dataset S4;* Figure S2). An increase in deposition is observed over the sea and land near southern Japan during interprovincial trade, which is attributed to both imported emissions into the North China Plain (e.g., Hebei, Shandong) (*SI Dataset S4*) and the seasonal winds of the East Asian Monsoon. Meanwhile, wind shear over the region may contribute to greater deposition and amplify the increase (Figure S3a and S3d).

In the spring and summer months, the prevailing wind direction is from the Northwest Pacific to Siberia, the opposite direction of the wind in the autumn and winter

287 months (Figure S3b and S3c). The seasonal winds bring atmospheric Hg from inland
288 China (e.g., Henan, Gansu, Shaanxi, and Inner Mongolia) to downwind regions outside
289 the western terrestrial boundary, such as Mongolia. An increase in deposition occurs over
290 these downwind regions due to the imported emissions in inland China during
291 interprovincial trade (*SI Dataset S4;* Figure S2). Due to the seasonal winds, the decrease
292 in atmospheric outflow from the eastern terrestrial boundary of China in the spring and
293 summer months is weaker than that in autumn and winter months. This phenomenon
294 indicates that interprovincial trade reduces the Hg risks to foreign countries mainly in the
295 autumn and winter months. Finally, a decrease in deposition is found along the line of the
296 Yellow Sea, the Korean Peninsula, the Sea of Japan and northern Japan all the year round.
297 The westerlies of the Northern Hemisphere throughout the year may contribute to this
298 phenomenon, resulting in these regions as the most important regions benefitting from
299 Chinese interprovincial trade.
300
301 **3.3 Projected impacts of interprovincial trade**
302 A large potential impact of Chinese interprovincial trade on the changes of
303 atmospheric Hg outflow can be inferred. At present, the relocation of emissions
304 embodied in the net interprovincial trade (85.6 Mg $year^{-1}$) results in the transfer of
305 atmospheric outflow from the eastern terrestrial boundary to western terrestrial boundary
306 and a net decrease in the atmospheric outflow from the whole boundary. Subsequently,
307 atmospheric deposition of Chinese anthropogenic Hg decreases over neighboring seas
308 and lands outside the eastern terrestrial boundary, for example, −10.5% for Chinese
309 coastal seas and −2.2% for Japan-Korea, and increases over neighboring lands outside the

western terrestrial boundary (Figure 4). These changes in outflow and deposition can be amplified with an increase in net interprovincial trade.

In addition to the emissions embodied in net interprovincial trade, the trade induces another 142.0 Mg year^{-1} of Hg emissions that is offset due to trade balance (Figure 4). Meanwhile, the consumption of local goods by the national population also induces 275.4 Mg year^{-1} of Hg emissions that are not involved in interprovincial trade (*SI Dataset S4*; Figure 4). If the interprovincial trade is strengthened in the future, the original trade balance would be broken and the consumption of local goods would be transferred to the consumption of imported goods. Then, the emissions embodied in net interprovincial trade would become larger, which would further promote the transfer of atmospheric outflow from the eastern terrestrial boundary to western terrestrial boundary and a net decrease in the atmospheric outflow from the whole boundary given the premise of constant total anthropogenic emissions. This change will further reduce the MeHg exposure risks to humans who live in the regions outside the eastern terrestrial boundary of China and those who rely heavily on the marine-based diets. For instance, Japan-Korea totally receives 6.3 Mg year^{-1} Hg from Chinese anthropogenic emissions. If the decrease responded proportionally to the increase of net interprovincial trade from 85.6 Mg year^{-1} to 503.0 Mg year^{-1}, we would expect a decrease of Chinese anthropogenic Hg from 6.3 Mg year^{-1} to 5.5 Mg year^{-1} deposited in Japan-Korea. That is, the maximum for transboundary impacts of China on Japan-Korea can be reduced by 11%, which is equivalent to the emission ratios of some critical emission sectors in China (e.g., coal-fired power plants). In general, a further reduction in transboundary Hg pollution from China is projected with the increase in net interprovincial trade.

333

334 **3.4 Policy implications of transboundary Hg controls**

335 Policies on Chinese anthropogenic sources would contribute considerably to the
336 mitigation of Hg-related health risks in Chinese neighboring regions in consideration of
337 the considerable atmospheric Hg outflow. The mitigation would vary between seasons,
338 with more mitigation occurring in the winter months due to the larger atmospheric Hg
339 outflow in those months. Chinese interprovincial trade promotes the transfer of
340 atmospheric outflow from the eastern terrestrial boundary to western terrestrial boundary,
341 and a net decrease in the atmospheric outflow from the whole boundary and increase in
342 the atmospheric deposition over terrestrial China. The decrease in deposition over
343 neighboring regions outside the eastern terrestrial boundary is more remarkable in the
344 autumn and winter months. Rapid industrialization and urbanization have substantially
345 increased the consumption of goods and services and associated interprovincial trade in
346 the past decades in China.[25] This change reveals that a considerable portion of Hg from
347 Chinese human activities has not been transported outside the eastern terrestrial boundary
348 and has been deposited in terrestrial China or transported outside the western terrestrial
349 boundary due to increasing interprovincial trade in the past decades. Chinese
350 interprovincial trade, to some extent, has offset the adverse effects of increasing
351 anthropogenic Hg emissions from China on neighboring seas and lands outside the
352 eastern terrestrial boundary of China.

353 Since the 11th Five-Year Plan, the Chinese government has committed to build and
354 develop urban agglomerations, which calls for more domestic consumption and domestic
355 imports. More domestic consumption and imports promote more emissions embodied in

356 interprovincial trade, which will flow from coastal developed urban agglomerations to
357 inland developing regions in the future. The projected increase in interprovincial trade is
358 expected to promote the transfer of atmospheric outflow from the eastern terrestrial
359 boundary to western terrestrial boundary and the further reduction in transboundary Hg
360 pollution from China. Alongside with the Hg controls implemented in China,
361 interprovincial trade has a synergistic promotional effect on the reduction in atmospheric
362 outflow, especially for the reduction in atmospheric deposition over regions outside the
363 eastern terrestrial boundary of China. Thus, the combination of Hg controls and
364 interprovincial trade could be considered to reduce the transboundary Hg pollution from
365 China.
366
367 **3.5 Uncertainties and recommendations**
368 Our model results are subject to uncertainties from various sources, including the
369 compilation of production-based emissions, the calculation of trade-induced emissions,
370 and the simulation of the atmospheric chemical transport model. Since the production-
371 based anthropogenic emissions from China are referenced from our previous work,[28] an
372 overall uncertainty of [−25.0%, 29.0%] from that study is used in this study. These
373 uncertainties are derived from knowledge gaps on Hg concentrations in fuel/raw
374 materials, Hg removal efficiencies and activity rates. The calculation of trade-induced
375 emissions includes an additional uncertainty from the MRIO analyses, which was
376 estimated to be 13.0% according to previous studies.[22,43,44] These uncertainties are
377 derived from knowledge gaps in economic statistics, sectoral mapping and data
378 harmonization.[45,46] The simulation of the atmospheric chemical transport model is subject

379 to errors in emission inputs and the model representation of tropospheric physical and
380 chemical processes. However, performing Monte Carlo and other sensitivity simulations
381 that require high computational costs is computationally prohibitive. Instead, we use the
382 normalized root-mean-square deviation (NRMSD) between the simulated and observed
383 results of atmospheric deposition to represent the uncertainties on the model in terms of
384 the method presented in Zhang et al.[44] Based on the method and the model evaluations in
385 our previous work,[28] the NRMSD is estimated to be 23.1% for atmospheric Hg
386 simulation over the model domain in 2010. In summary, based on the aggregation of the
387 uncertainties above, we estimate an overall uncertainty of [−34.1%, 37.1%] for
388 atmospheric deposition and outflow in Section 3.1 and [−36.4%, 39.3%] for changes in
389 atmospheric deposition and outflow in Section 3.2.

390 The MRIO database used in this study is derived from Liu et al.,[29] while many other
391 MRIO databases have been developed for China, such as those developed by Shi and
392 Zhang,[47] Zhang and Qi,[48] and Wang et al.[49,50] Especially, Wang et al.[49,50] have recently
393 developed a more resolution-detailed and time-detailed MRIO database for China, which
394 also comes with accompanying standard deviation tables. The use of the database from
395 Liu et al.[29] makes it easy to compare our results to those of most previous studies that
396 used the database, and it will be critical and possible to compare and harmonize the
397 results based on the other databases in future studies. Meanwhile, to evaluate the impacts
398 of interprovincial trade on atmospheric deposition over neighboring regions, we choose
399 several representative neighboring seas and lands but do not include all neighboring
400 regions of China in this study. Through additional measurements and models of the
401 marine Hg cycle and diet habits of humans, the evaluation of human MeHg exposure

risks from the consumption of seafood harvested from marine regions outside the eastern terrestrial boundary of China would assist further analysis of this subject in the future. Moreover, transboundary Hg pollution has interactional impacts between China and neighboring countries. We investigate the impacts of Chinese emissions on neighboring countries from the perspective of interprovincial trade in this study. The impacts of emissions from neighboring countries on China need to be studied from the perspective of international trade in the future.

409 **Author Information**

410 **Corresponding Authors**

411 *(J.S.) Phone: +86-21-54341198; e-mail: jshu@geo.ecnu.edu.cn.

412 *(X.W.) Phone: +86-10-62759190; e-mail: xjwang@urban.pku.edu.cn.

413

414 **Acknowledgments**

415 The authors would like to thank the editor and anonymous reviewers for their thoughtful
416 comments. This study was funded by the National Natural Science Foundation of China
417 (41701589, 41630748, 41271055), and China Postdoctoral Science Foundation Grant
418 (2017M611492, 2018T110372). Sai Liang thanks the financial support of the
419 Fundamental Research Funds for the Central Universities and Interdiscipline Research
420 Funds of Beijing Normal University. All map images are plotted by GAMAP (Global
421 Atmospheric Model Analysis Package, Version 2.17;
422 http://acmg.seas.harvard.edu/gamap/). The computation was supported by the High
423 Performance Computer Center of East China Normal University.

424

425 **Supporting Information**

426 Additional information on study domain and boundaries for regional definitions (Figure
427 S1; Dataset S1), net emission flows induced by interprovincial trade in 2010 (Figure S2),
428 seasonal distribution of wind speed and wind direction over East Asian domain in 2010
429 (Figure S3), sector classification of the Chinese MRIO table and allocation of emissions
430 in this study (Datasets S2 and S3), provincial production-based and trade-induced
431 emissions and associated sector-specified data in 2010 (Datasets S4 and S5).

Reference

1 Arctic Monitoring and Assessment Programme and United Nations Environment Programme (AMAP/UNEP). *Technical Background Report for the Global Mercury Assessment*; AMAP/UNEP: Geneva, Switzerland, 2013.

2 Corbitt, E. S.; Jacob, D. J.; Holmes, C. D.; Streets, D. G.; Sunderland, E. M. Global source-receptor relationships for mercury deposition under present-day and 2050 emissions scenarios. *Environ. Sci. Technol.* **2011**, *45* (24), 10477–10484.

3 Harris, R. C.; Rudd, J. W. M.; Amyot, M.; Babiarz, C. L.; Beaty, K. G.; Blanchfield, P. J.; Bodaly, R. A.; Branfireun, B. A.; Gilmour, C. C.; Graydon, J. A. Whole-ecosystem study shows rapid fish-mercury response to changes in mercury deposition. *Proc. Natl. Acad. Sci. U. S. A.* **2007**, *104* (42), 16586–16591.

4 Vijayaraghavan, K.; Levin, L.; Parker, L.; Yarwood, G.; Streets, D. Response of fish tissue mercury in a freshwater lake to local, regional, and global changes in mercury emissions. *Environ. Toxicol. Chem.* **2014**, *33* (6), 1238–1247.

5 Roman, H. A.; Walsh, T. L.; Coull, B. A.; Dewailly, É.; Guallar, E.; Hattis, D.; Mariën, K.; Schwartz, J.; Stern, A. H.; Virtanen, J. K. Evaluation of the cardiovascular effects of methylmercury exposures: Current evidence supports development of a dose–response function for regulatory benefits analysis. *Environ. Health Persp.* **2011**, *119* (5), 607–614.

452 6 Grandjean, P.; Satoh, H.; Murata, K.; Eto, K. Adverse effects of methylmercury:
453 Environmental health research implications. *Environ. Health Persp.* **2010**, *118*
454 (8), 1137–1145.

455 7 Karagas, M. R.; Choi, A. L.; Oken, E.; Horvat, M.; Schoeny, R.; Kamai, E.;
456 Cowell, W.; Grandjean, P.; Korrick, S. Evidence on the human health effects of
457 low-level methylmercury exposure. *Environ. Health Persp.* **2012**, *120* (6), 799–
458 806.

459 8 National Institude for Minamata Disease (NIMD), Ministry of the Environment.
460 *Minamata disease archives*, http://www.nimd.go.jp/english/.

461 9 United Nations Environment Programme (UNEP). *Minamata Convention on*
462 *Mercury*, http://www.mercuryconvention.org.

463 10 Zhang, L.; Wang, S.; Wang, L.; Wu, Y.; Duan, L.; Wu, Q.; Wang, F.; Yang, M.;
464 Yang, H.; Hao, J. Updated emission inventories for speciated atmospheric
465 mercury from anthropogenic sources in China. *Environ. Sci. Technol.* **2015**, *49*
466 (5), 3185–3194.

467 11 Wu, Q.; Wang, S.; Li, G.; Liang, S.; Lin, C. J.; Wang, Y.; Cai, S.; Liu, K.; Hao, J.
468 Temporal trend and spatial distribution of speciated atmospheric mercury
469 emissions in China during 1978–2014. *Environ. Sci. Technol.* **2016**, *50* (24),
470 13428–13435.

471 12 Ogawa, S.; Okochi, H.; Ogata, H.; Umezawa, N.; Miura, K.; Kato, S. Observation
472 of gaseous elemental mercury (GEM) in the free troposphere at Mt. Fuji: Summer

observational campaign in 2014. *J. Japan Soci. Atmos. Environ.* **2015**, *50*, 100–106.

13 Nagafuchi, O.; Yokota, K.; Kato, S.; Osaka, K. I.; Nakazawa, K.; Koga, M.; Hishida, N.; Nishida, Y. Origin of atmospheric gaseous mercury using the Hg/CO ratio in pollution plume observed at Mt. Fuji Weather Station; *Japan Geoscience Union Meeting 2014*: Pacifico Yokohama, Kanagawa, Japan, 28 April–02 May 2014.

14 Jaffe, D.; Prestbo, E.; Swartzendruber, P.; Weiss-Penzias, P.; Kato, S.; Takami, A.; Hatakeyama, S.; Kajii, Y. Export of atmospheric mercury from Asia. *Atmos. Environ.* **2005**, *39* (17), 3029–3038.

15 Sprovieri, F.; Pirrone, N.; Ebinghaus, R.; Kock, H.; Dommergue, A. A review of worldwide atmospheric mercury measurements. *Atmos. Chem. Phys.* **2010**, *10*, 8245–8265.

16 Lin, C. J.; Pan, L.; Streets, D. G.; Shetty, S. K.; Jang, C.; Feng, X.; Chu, H. W.; Ho, T. C. Estimating mercury emission outflow from East Asia using CMAQ-Hg. *Atmos. Chem. Phys.* **2010**, *10* (4), 1853–1864.

17 Pan, L.; Lin, C. J.; Carmichael, G. R.; Streets, D. G.; Tang, Y.; Woo, J. H.; Shetty, S. K.; Chu, H. W.; Ho, T. C.; Friedli, H. R. Study of atmospheric mercury budget in East Asia using STEM-Hg modeling system. *Sci. Total Environ.* **2010**, *408* (16), 3277–3291.

18 Chen, L.; Wang, H. H.; Liu, J. F.; Tong, Y. D.; Ou, L. B.; Zhang, W.; Hu, D.; Chen, C.; Wang, X. J. Intercontinental transport and deposition patterns of

atmospheric mercury from anthropogenic emissions. *Atmos. Chem. Phys.* **2014**, *13* (9), 25185–25218.

19 Durnford, D.; Dastoor, A.; Figueras-Nieto, D.; Ryjkov, A. Long range transport of mercury to the Arctic and across Canada. *Atmos. Chem. Phys.* **2010**, *10*, 6063–6086.

20 Pirrone, N.; Keating, T. *Hemispheric Transport of Air Pollution 2010, Part B: Mercury*; United Nations Publication: Geneva, Switzerland, 2011.

21 Wang, H.; Zhang, Y.; Zhao, H.; Lu, X.; Zhang, Y.; Zhu, W.; Nielsen, C. P.; Li, X.; Zhang, Q.; Bi, J. Trade-driven relocation of air pollution and health impacts in China. *Nat. Commun.* **2017**, *8* (1), 738.

22 Peters, G. P.; Davis, S. J.; Andrew, R. A synthesis of carbon in international trade. *Biogeosciences* **2012**, *9*, 3247–3276.

23 Feng, K.; Davis, S. J.; Sun, L.; Li, X.; Guan, D.; Liu, W.; Liu, Z.; Hubacek, K. Outsourcing CO_2 within China. Proc. *Natl. Acad. Sci. U. S. A.* **2013**, *110* (28), 11654–11659.

24 Hui, M.; Wu, Q.; Wang, S.; Liang, S.; Zhang, L.; Wang, F.; Lenzen, M.; Wang, Y.; Xu, L.; Lin, Z. Mercury flows in China and global drivers. *Environ. Sci. Technol.* **2017**, *51* (1), 222–231.

25 Liang, S.; Xu, M.; Liu, Z.; Suh, S.; Zhang, T. Socioeconomic drivers of mercury emissions in China from 1992 to 2007. *Environ. Sci. Technol.* **2013**, *47* (7), 3234–3240.

516 26 Liang, S.; Chao, Z.; Wang, Y.; Ming, X.; Liu, W. Virtual atmospheric mercury
517 emission network in China. *Environ. Sci. Technol.* **2014**, *48* (5), 2807–2815.

518 27 Li, J. S.; Chen, G. Q.; Chen, B.; Yang, Q.; Wei, W. D.; Wang, P.; Dong, K. Q.;
519 Chen, H. P. The impact of trade on fuel-related mercury emissions in Beijing–
520 evidence from three-scale input-output analysis. *Renew. Sust. Energ. Rev.* **2017**,
521 *75*, 742–752.

522 28 Chen, L.; Meng, J.; Liang, S.; Zhang, H.; Zhang, W.; Liu, M.; Tong, Y.; Wang,
523 H.; Wang, W.; Wang, X.; Shu, J. Trade-induced atmospheric mercury deposition
524 over China and implications for demand-side controls. *Environ. Sci. Technol.*
525 **2018**, *52* (4), 2036–2045.

526 29 Liu, W. D.; Tang, Z. P.; Chen, J.; Yang, B. *China's interregional input−output*
527 *table for 30 regions in 2010 (in Chinese)*; China Statistics Press: Beijing, China,
528 2014.

529 30 Peters, G. P.; Weber, C. L.; Guan, D.; Hubacek, K. China's growing CO_2
530 emissions–a race between increasing consumption and efficiency gains. *Environ.*
531 *Sci. Technol.* **2007**, *41* (17), 5939–5944.

532 31 Weber, C. L.; Peters, G. P.; Guan, D.; Hubacek, K. The contribution of Chinese
533 exports to climate change. *Energy Policy* **2008**, *36* (9), 3572–3577.

534 32 Selin, N. E.; Jacob, D. J.; Park, R. J.; Yantosca, R. M.; Strode, S.; Jaeglé, L.;
535 Jaffe, D. Chemical cycling and deposition of atmospheric mercury: Global
536 constraints from observations. *J. Geophys. Res. Atmos.* **2007**, *112* (D2), 557–573.

537 33 Holmes, C. D.; Jacob, D. J.; Corbitt, E. S.; Mao, J.; Yang, X.; Talbot, R.; Slemr,
538 F. Global atmospheric model for mercury including oxidation by bromine atoms.
539 *Atmos. Chem. Phys.* **2010**, *10* (24), 12037–12057.

540 34 Soerensen, A. L.; Sunderland, E. M.; Holmes, C. D.; Jacob, D. J.; Yantosca, R.
541 M.; Skov, H.; Christensen, J. H.; Strode, S. A.; Mason, R. P. An improved global
542 model for air-sea exchange of mercury: High concentrations over the North
543 Atlantic. *Environ. Sci. Technol.* **2010**, *44* (22), 8574–8580.

544 35 Amos, H. M.; Jacob, D. J.; Holmes, C. D.; Fisher, J. A.; Wang, Q.; Yantosca, R.
545 M.; Corbitt, E. S.; Galarneau, E.; Rutter, A. P.; Gustin, M. S.; Steffen, A.;
546 Schauer, J. J.; Graydon, J. A.; Louis, V. L. S.; Talbot, R. W.; Edgerton, E. S.;
547 Zhang, Y.; Sunderland, E. M. Gas-particle partitioning of atmospheric Hg(II) and
548 its effect on global mercury deposition. *Atmos. Chem. Phys.* **2012**, *12* (1), 591–
549 603.

550 36 Wesely, M. L. Parameterization of surface resistances to gaseous dry deposition
551 in regional-scale numerical models. *Atmos. Environ.* **1989**, *23*, 1293–1304.

552 37 Liu, H.; Jacob, D. J.; Bey, I.; Yantosca, R. M. Constraints from 210Pb and 7Be on
553 wet deposition and transport in a global three-dimensional chemical tracer model
554 driven by assimilated meteorological fields. *J. Geophys. Res. Atmos.* **2001**, *106*,
555 12109–12128.

556 38 Mergler, D.; Anderson, H. A.; Chan, L. H. M.; Mahaffey, K. R.; Murray, M.;
557 Sakamoto, M.; Stern, A. H. Methylmercury exposure and health effects in
558 humans: A worldwide concern. *Ambio* **2007**, *36* (1), 3–11.

559 39 Selin, N. E.; Sunderland, E. M.; Knightes, C. D.; Mason, R. P. Sources of
560 mercury exposure for U.S. seafood consumers: Implications for policy. *Environ.*
561 *Health Persp.* **2010**, *118*, 137–143.

562 40 Mahaffey, K. R.; Sunderland, E. M.; Chan, H. M.; Choi, A. L.; Grandjean, P.;
563 Mariën, K.; Oken, E.; Sakamoto, M.; Schoeny, R.; Weihe, P.; Yan, C.-H.;
564 Yasutake, A. Balancing the benefits of n-3 polyunsaturated fatty acids and the
565 risks of methylmercury exposure from fish consumption. *Nut. Rev.* **2011**, *69* (9),
566 493–508.

567 41 Sunderland, E. M. Mercury exposure from domestic and imported estuarine and
568 marine fish in the U.S. seafood market. *Environ. Health Persp.* **2007**, *115*, 235–
569 242.

570 42 Sunderland, E. M.; Mason, R. P. Human impacts on open ocean mercury
571 concentrations. *Global Biogeochem. Cy.* **2007**, *21*, 177–180.

572 43 Lin, J.; Tong, D.; Davis, S.; Ni, R.; Tan, X.; Pan, D.; Zhao, H.; Lu, Z.; Streets, D.;
573 Feng, T.; Zhang, Q.; Yan, Y.; Hu, Y.; Li, J.; Liu, Z.; Jiang, X.; Geng, G.; He, K.;
574 Huang, Y.; Guan, D. Global climate forcing of aerosols embodied in international
575 trade. *Nat. Geosci.* **2016**, *9* (10), 790–794.

576 44 Zhang, Q.; Jiang, X.; Tong, D.; Davis, S. J.; Zhao, H.; Geng, G.; Feng, T.; Zheng,
577 B.; Lu, Z.; Streets, D. G.; Ni, R.; Brauer, M.; Donkelaar, A. V.; Martin, R. V.;
578 Huo, H.; Liu, Z.; Pan, D.; Kan, H.; Yan, Y.; Lin, J.; He, K.; Guan, D.
579 Transboundary health impacts of transported global air pollution and international
580 trade. *Nature* **2017**, *543* (7647), 705.

581 45 Lenzen, M.; Moran, D.; Kanemoto, K.; Foran, B.; Lobefaro, L.; Geschke, A.
582 International trade drives biodiversity threats in developing nations. *Nature* **2012**,
583 *486* (7401), 109–112.

584 46 Steenolsen, K.; Owen, A.; Barrett, J.; Guan, D.; Hertwich, E. G.; Lenzen, M.;
585 Wiedmann, T. Accounting for value added embodied in trade and consumption:
586 An intercomparison of global multiregional input–output databases. *Econ. Syst.*
587 *Res.* **2016**, *28* (1), 78–94.

588 47 Shi, J.; Zhang, Z. *Inter-province input-output model and interregional economic*
589 *linkage in China (in Chinese)*; Science Press: Beijing, China, 2012.

590 48 Zhang, Y.; Qi, S. *China multi-regional input-output models(in Chinese)*; China
591 Statistics Press: Beijing, China, 2012.

592 49 Wang, Y.; Geschke, A.; Lenzen, M. Constructing a time series of nested
593 multiregion input-output tables. *Int. Reg. Sci. Rev.* **2017**, 40 (5), 476–499.

594 50 Wang, Y. An industrial ecology virtual framework for policy making in China.
595 *Econ. Syst. Res.* **2017**, *29* (2), 252–274.
596

Figure Captions

Figure 1. Spatial distribution of atmospheric Hg deposition over East Asia driven by Chinese anthropogenic emissions (a) and the Hg mass budget for China (b). The season "winter" includes December (D), January (J), and February (F). The season "spring" includes March (M), April (A), and May (M). The season "summer" includes June (J), July (J), and August (A). The season "autumn" includes September (S), October (O), and November (N). The mass budget includes atmospheric emissions, atmospheric deposition, atmospheric burden, and atmospheric outflow.

Figure 2. Changes in the spatial distribution of atmospheric Hg deposition over East Asia (a) and changes in the Hg mass budget for China (b) as driven by Chinese interprovincial trade.

Figure 3. Changes in the spatial distribution of atmospheric Hg deposition over East Asia except for terrestrial China as driven by Chinese interprovincial trade. The definitions of the seasons are the same as those for Figure 1. The number in blue color located in the lower left corner of each panel indicates the sum of decreasing global atmospheric deposition driven by Chinese interprovincial trade (unit: Mg season^{-1}), and the number in red color indicates the sum of increasing global atmospheric deposition driven by Chinese interprovincial trade (unit: Mg season^{-1}).

Figure 4. Changes in the atmospheric Hg budget for China and the atmospheric Hg deposition over neighboring seas and lands driven by trade-induced emissions of China. The total national anthropogenic emissions consist of emissions from each province, including the emissions embodied in the consumption of local goods, consumption of imported goods and other emissions (e.g., residential coal consumption and the use of Hg-added products). The "net" emissions represent the emissions embodied in net interprovincial trade. The unit of all the numbers except numbers in parentheses is Mg year^{-1}. The numbers in parentheses represent the proportion of the change induced by interprovincial trade to total deposition of Chinese anthropogenic Hg over each neighboring region. The definition of each neighboring region is described in *SI Dataset S1*, and the Chinese coastal seas include the Bohai Sea, Yellow Sea, East China Sea, and South China Sea.

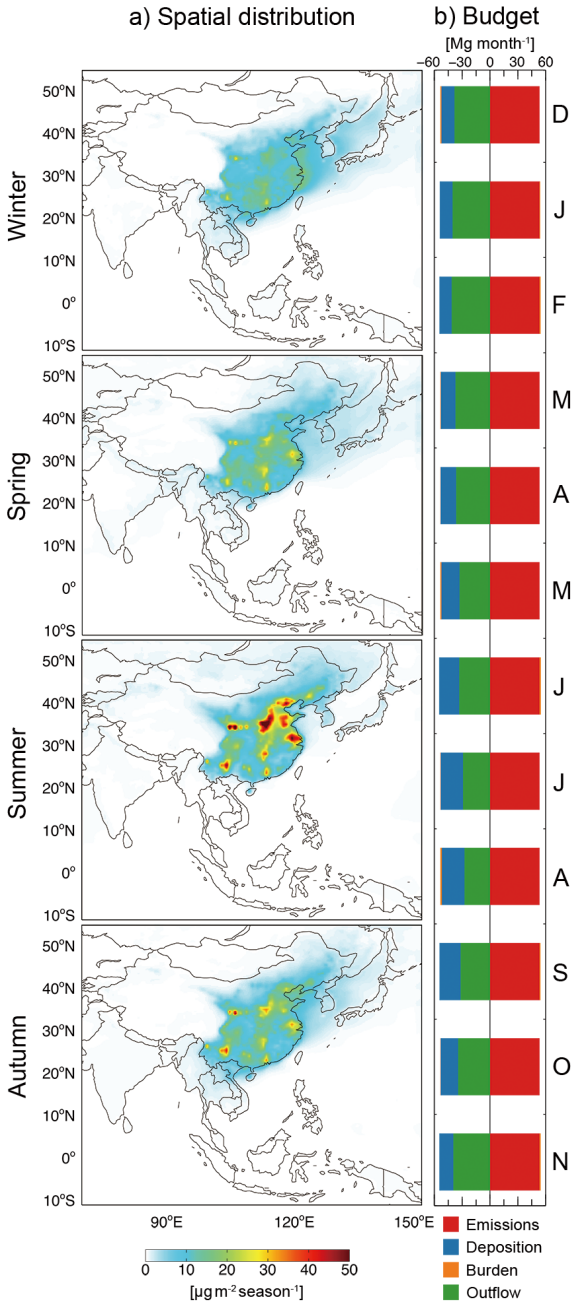

Figure 1. Spatial distribution of atmospheric Hg deposition over East Asia driven by Chinese anthropogenic emissions (a) and the Hg mass budget for China (b). The season "winter" includes December (D), January (J), and February (F). The season "spring" includes March (M), April (A), and May (M). The season "summer" includes June (J), July (J), and August (A). The season "autumn" includes September (S), October (O), and November (N). The mass budget includes atmospheric emissions, atmospheric deposition, atmospheric burden, and atmospheric outflow.

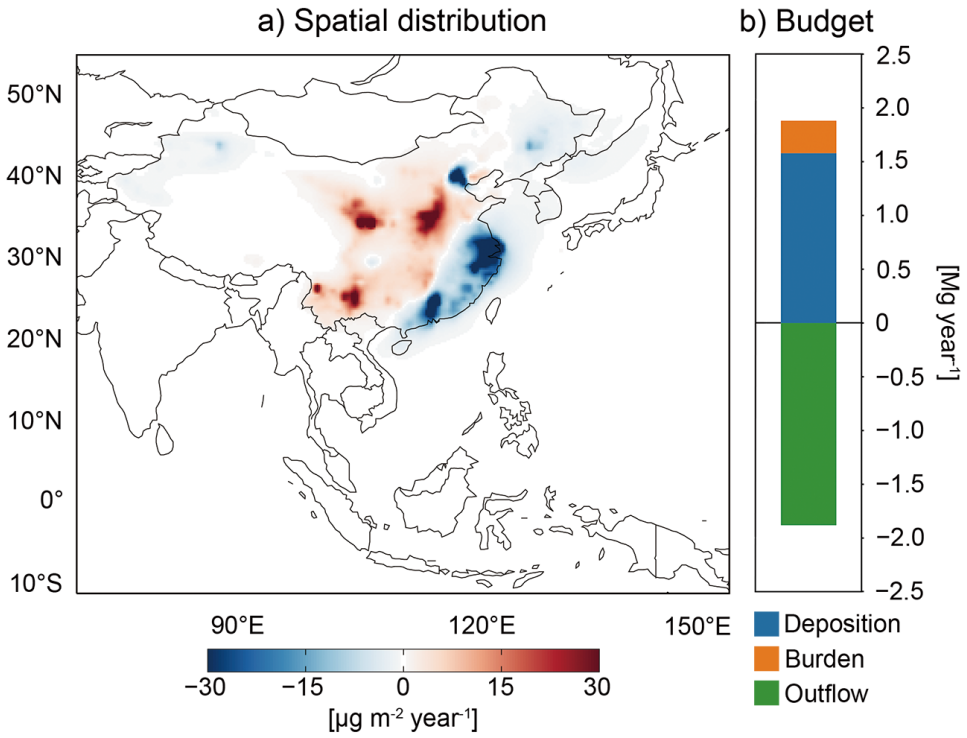

Figure 2. Changes in the spatial distribution of atmospheric Hg deposition over East Asia (a) and changes in the Hg mass budget for China (b) as driven by Chinese interprovincial trade.

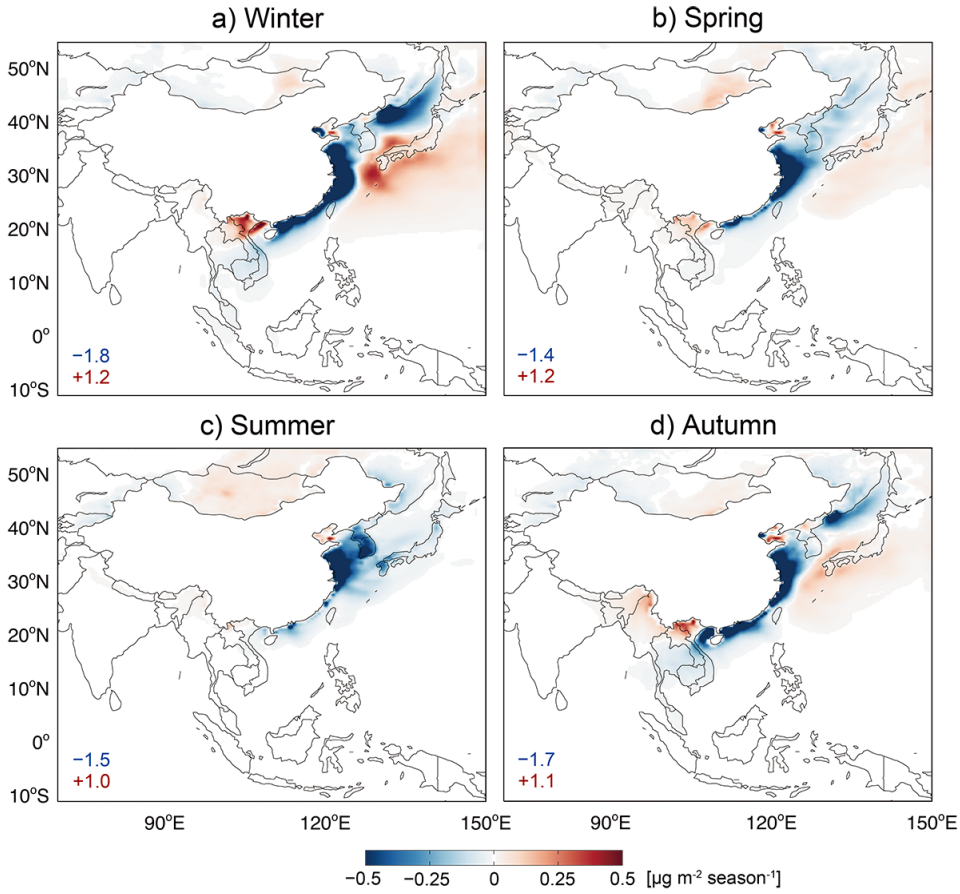

Figure 3. Changes in the spatial distribution of atmospheric Hg deposition over East Asia except for terrestrial China as driven by Chinese interprovincial trade. The definitions of the seasons are the same as those for Figure 1. The number in blue color located in the lower left corner of each panel indicates the sum of decreasing global atmospheric deposition driven by Chinese interprovincial trade (unit: Mg season^{-1}), and the number in red color indicates the sum of increasing global atmospheric deposition driven by Chinese interprovincial trade (unit: Mg season^{-1}).

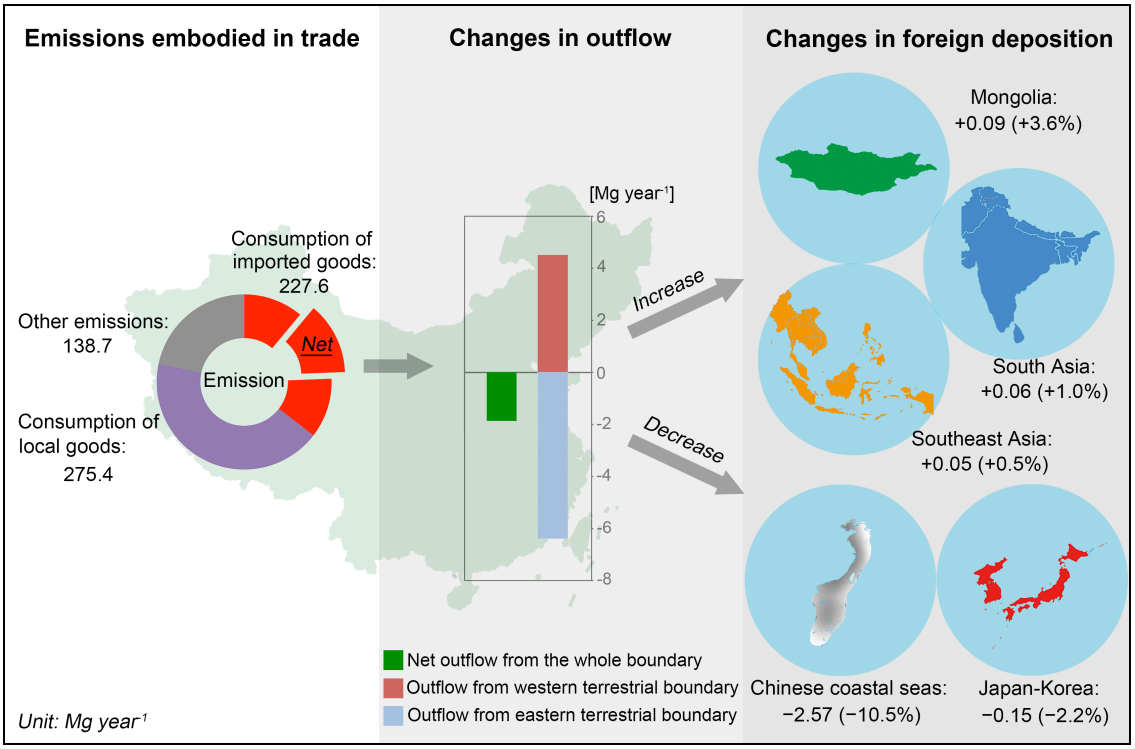

Figure 4. Changes in the atmospheric Hg budget for China and the atmospheric Hg deposition over neighboring seas and lands driven by trade-induced emissions of China. The total national anthropogenic emissions consist of emissions from each province, including the emissions embodied in the consumption of local goods, consumption of imported goods and other emissions (e.g., residential coal consumption and the use of Hg-added products). The "net" emissions represent the emissions embodied in net interprovincial trade. The unit of all the numbers except numbers in parentheses is Mg year^{-1}. The numbers in parentheses represent the proportion of the change induced by interprovincial trade to total deposition of Chinese anthropogenic Hg over each neighboring region. The definition of each neighboring region is described in *SI Dataset S1*, and the Chinese coastal seas include the Bohai Sea, Yellow Sea, East China Sea, and South China Sea.

69 **TOC/Abstract Art**

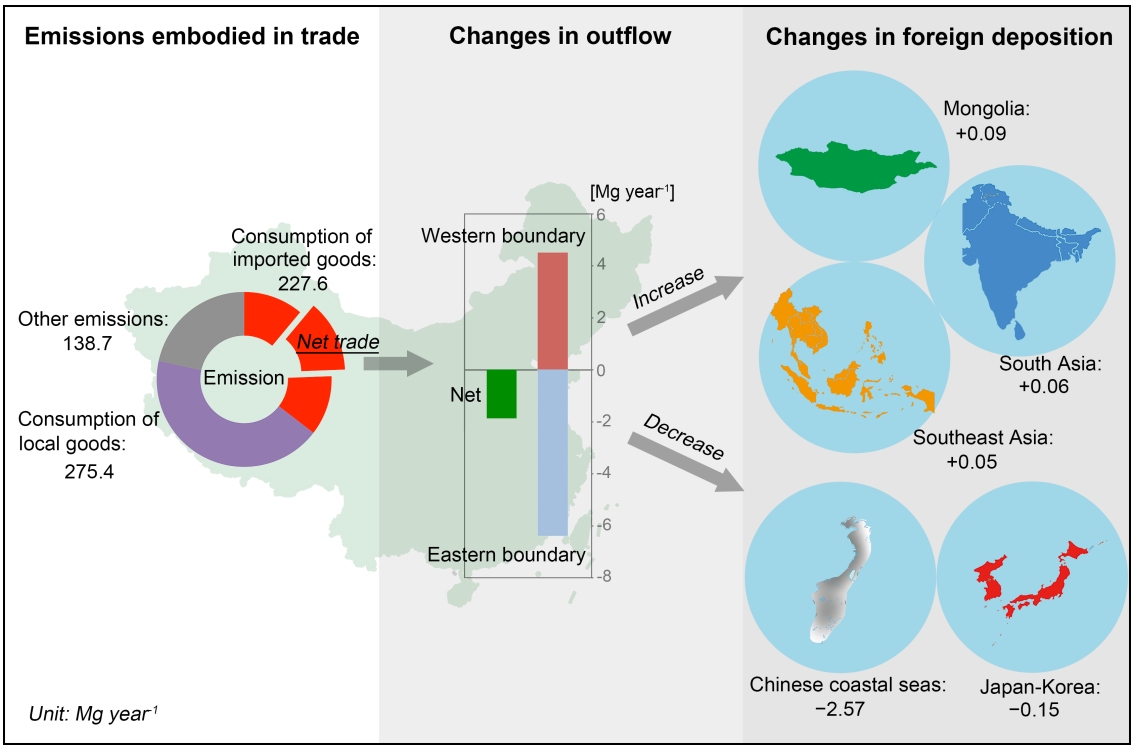

70